**Palestine Journal of Mathematics**

**Vol.15(3), (2026)** , 1300–1315 © Palestine Polytechnic University-PPU 2026

# Properties of finite continuous Radon and Ridgelet transform with its applications to Neural network and Klein-Gordon equations

N. Gupta and V. R. Lakshmi Gorty

Communicated by Geeta Arora

MSC 2020 Classifications: Primary 46F12; Secondary 44A20, 44A45.

Keywords and phrases: Finite continuous Radon transform, linear non-homogeneous equations, finite continuous Ridgelet transform, Klein-Gordon equation, neural network.

*The authors would like to thank the reviewers and editor for their constructive comments and valuable suggestions that improved the quality of our paper*

**Corresponding Author: N. Gupta**

**Abstract**. This paper presents the relationship between the finite continuous Radon and Ridgelet transforms. Both transforms are expressed in terms of the finite continuous Fourier transform. The paper also establishes fundamental properties such as linearity, shifting, scaling, and symmetry. In the concluding section, the relationship between the finite continuous Radon and Ridgelet transforms is applied to neural networks using the Mexican Hat wavelet. Additionally, the paper demonstrates an application to neural networks through graphical interpretations and the solution of two forms of the linear non-homogeneous Klein-Gordon equation with their respective initial conditions. Comparison tables and graphical representations of the Klein-Gordon equation solutions, obtained using the finite continuous Radon and Ridgelet transforms are also presented.

## 1 Introduction

### Ridgelet transform

The continuous Ridgelet transform for bivariate function $f(x,y)$ defined by Candès [2] as

$$\Re_f(a,b,\theta) = \int_{-\infty}^{\infty}\int_{-\infty}^{\infty} f(x,y)\,\psi_{a,b,\theta}(x,y)\,dxdy \tag{1.1}$$

where $\psi_{a,b,\theta}(x,y) = a^{-1/2}\,\psi\left[\frac{(x\cos\theta+y\sin\theta-b)}{a}\right]$ is a ridge function $\forall\ a>0,\ b\in\mathbb{R}$ and $\theta\in[0,2\pi)$ and $\psi_{a,b,\theta}:\mathbb{R}^2\to\mathbb{R}^2$.
Murata, in [9], independently studied and analyzed ridgelet integral representations. In 1998, Donoho [10] broadened the notion of ridgelets and studied orthonormal ridgelets whose elements can be specified in closed form. In [11], the author extended ridgelets to higher dimensions. The discrete finite ridgelet transform was introduced in 2003 by Do and Vetterli [13]. In [12], using the convolution of quaternion-valued functions, the authors defined the ridgelet transform on square-integrable quaternion-valued functions. The authors also conducted a series of computational experiments to show an interesting similarity between the scatter plot of hidden parameters in a shallow neural network after BP training and the spectrum of the ridgelet transform, as discussed in [14].
The classical work of finite continuous Ridgelet transforms was developed in [18], using Sturm-

Liouville theory [15, 17] as follows:

$$\Re_{p,q,a,b} f(x,y) = \frac{a^{-1/2}}{4\alpha\beta} \int_{-\beta}^{\beta} \int_{-\alpha}^{\alpha} f(x,y)\, \psi\left(\left((pa\pi x/\alpha) + (qa\pi y/\beta) - b\right)/a\right) dxdy. \tag{1.2}$$

The inversion formula of (1.2) is given by

$$\Re^{-1}\left(\Re_{p,q,a,b} f(x,y)\right) = a^{1/2} \sum_{p,q=1}^{\infty} \Re_{p,q,a,b} f(x,y)\, \psi\left(\left((pa\pi x/\alpha) + (qa\pi y/\beta) - b\right)/a\right) \tag{1.3}$$

where

$$\left(1 + \sum_{p,q=1}^{\infty} e^{-((pa\pi x/\alpha)+(qa\pi y/\beta)-b)/a}\right)^{-1} = \psi\left(\left((pa\pi x/\alpha) + (qa\pi y/\beta) - b\right)/a\right) \tag{1.4}$$

which is a ridge function or ridgelet with parameters:
i) $a$; the scale of the ridge function
ii) $b$; location of the ridge function
iii) $[(pa\pi x/\alpha) + (qa\pi y/\beta)]$; its orientation.

## Radon transform

How to construct a function of two variables from its integrals over all straight lines in the plane was demonstrated by Johann Radon [1] in 1917 and was defined as

$$\hat{f}(P,\phi) = R\{f(x,y)\} = \int_{-\infty}^{\infty} \int_{-\infty}^{\infty} f(x,y)\, \delta(P - x\cos\theta - y\sin\theta)\, dxdy \tag{1.5}$$

where $\delta(\cdot)$ is Dirac delta function ($\delta(x) = 1$ if $x = 0$ and 0 elsewhere), $\theta \in [0,\pi]$ and $P = x\cos\theta - y\sin\theta$ as $P \in [-\infty,\infty]$.
The exponential Radon transform, a generalization of the Radon transform, was defined as a mapping between function spaces in [3]. In [4], the author presented a summary of the fundamental properties of the continuous Radon transform, including delay effects, data shifting, rotation, scaling, windowing, bowtie events, and energy conservation. The paper also includes representative examples on standard datasets such as 2D delta functions, boxcar events, Gaussian bells, and conic sections, which help reinforce the basic concepts of the Radon transform. In [5], author studied an unbounded realization of the classical domain of type one. In this article, author defined the Radon transform on $\mathbb{R}$ and obtained an inversion formula $\mathbb{R} - 1 = (pi)(-2d)LRL$ in terms of a determinantal differential operator. In [6], the author formulated conditions for the finite-type Radon transform, which, modulo endpoints, lead to regularity properties in two dimensions. Numerical integration of finite Radon transforms over various function classes in multiple dimensions was studied in [7]. In [8], the relationship between the moments of the Radon transform and those of its modified version was derived. The author used modified Radon transform data to provide a uniform approximation of the original density function. A reconstruction algorithm was then implemented, and a simple density function was reconstructed from the moments of its modified Radon transform. This paper presents the relationship between the finite continuous Radon transform, the finite continuous Ridgelet transform, and wavelets, analogous to the approach in [11]. Both the finite continuous Radon and Ridgelet transforms are also expressed in terms of the finite continuous Fourier transform, as in [3]. The fundamental properties of the finite continuous Radon and Ridgelet transforms—such as linearity, shifting, scaling, and symmetry—are summarized, in line with the discussion in [4].

The wavelet lifting scheme is developed in [25] to obtain solutions of hyperbolic differential equations that arise in mathematical physics. The study in [26] introduces the Sum transform

and explores its properties and applications in solving differential equations. The study [27] discusses methods for solving generalized differential equations through a generalized integral transform. The concluding section applies the relationship between the finite continuous Radon and Ridgelet transforms within a neural network model using the Mexican Hat wavelet. The application of these transforms is further extended to obtain solutions to two different forms of the linear non-homogeneous Klein-Gordon equation using given initial conditions. Finally, classical results concerning Klein–Gordon–Maxwell-type systems are briefly reviewed, as in [23].

## 2 Preliminary results (The Fourier-Radon series and finite continuous Radon transformation)

Assume $f(x,y)$ is a square integrable function over rectangle such that if $l,k$ are real constants and $\{(x,y) : -k < x < k, -l < y < l\}$ then

$$f(x,y) = c_{m,n}\left[1 + 2\sum_{m,n=1}^{\infty} \cos\pi\left(P - \frac{m}{k}x - \frac{n}{l}y\right)\right] \tag{2.1}$$

where $m,\ n,\ P \in \mathbb{R}$ and $c_{m,n}$ is constant. Using [24], multiplying (2.1)by $\left[1 + 2\cos\pi\left(P - \frac{m}{k}x - \frac{n}{l}y\right)\right]$ and integrating w.r.t $x,\ y$ over $[-k,k]$, $[-l,l]$ analogous [15, p. 122-124] yields:

$$c_{m,n} = \frac{1}{8kl}\int_{-l}^{l}\int_{-k}^{k} f(x,y)\left[1 + 2\sum_{m,n=1}^{\infty} \cos\pi\left(P - \frac{m}{k}x - \frac{n}{l}y\right)\right]dxdy. \tag{2.2}$$

From [19, p. 65], $\left[1 + 2\sum_{m,n=1}^{\infty} \cos\pi\left(P - \frac{m}{k}x - \frac{n}{l}y\right)\right]$ represents the regularized Dirac delta function and can be denoted as [22];

$$\left[1 + 2\sum_{m,n=1}^{\infty} \cos\pi\left(P - \frac{m}{k}x - \frac{n}{l}y\right)\right] = \delta\left(\pi\left(P - \frac{m}{k}x - \frac{n}{l}y\right)\right). \tag{2.3}$$

Hence (2.2) becomes

$$c_{m,n} = \frac{1}{8kl}\int_{-l}^{l}\int_{-k}^{k} f(x,y)\,\delta\left(\pi\left(P - \frac{m}{k}x - \frac{n}{l}y\right)\right)dxdy. \tag{2.4}$$

The convergence of the series (2.3) is straightforward by [17, p. 433] and [19, p. 63].

**Remark 2.1.** The finite continuous Radon transform analogous to [17, p. 425] as follows:

$$R_{m,n,P}f(x,y) = \frac{1}{8kl}\int_{-l}^{l}\int_{-k}^{k} f(x,y)\,\delta\left(\pi\left(P - \frac{m}{k}x - \frac{n}{l}y\right)\right)dxdy \tag{2.5}$$

Inversion formula of (2.5) is given by

$$R^{-1}\left(R_{m,n,P}f(x,y)\right) = f(x,y) = \sum_{m,n=1}^{\infty} R_{m,n,P}f(x,y)\ \delta\left(\pi\left(P - \frac{m}{k}x - \frac{n}{l}y\right)\right). \tag{2.6}$$

We point out the following operational rules if $f(x,y)$ is zero at boundary:

$$R_{m,n,P}\left\{\frac{\partial^2 f}{\partial x^2}\right\} = -\left(\frac{m\pi}{k}\right)^2 R_{m,n,P}f(x,y). \tag{2.7}$$

$$R_{m,n,P}\left\{\frac{\partial^2 f}{\partial y^2}\right\} = -\left(\frac{n\pi}{l}\right)^2 R_{m,n,P}f(x,y). \tag{2.8}$$

## 3 Relations between finite continuous Radon, Ridgelet and Fourier cosine transform

### 3.1 Relation between finite continuous Radon and Ridgelet transform

**Theorem 3.1.** *Let* $f \in L^1\left(\mathbb{R}^2\right)$. *Let* $R_{m,n,P}f\,(x,y)$ *and* $\Re_{p,q,a,b}f\,(x,y)$ *be defined on* $f\,(x,\,y)$ *as in* (2.5) *and* (1.2), *then*

$$\left\langle R_{m,n,P}f\,(x,y)\,,\ \psi_{a,\,b}\,(P)\right\rangle\ =\frac{\pi}{2}\Re_{p/\pi a,q/\pi a,a,b}f\,(x,y) \tag{3.1}$$

*where* $\psi_{a,\,b}\,(t)$ *is a wavelet.*

*Proof.* Consider

$$\left\langle R_{m,n,P}f\,(x,y)\,,\ \psi_{a,\,b}\,(P)\right\rangle$$

$$=\int_{-\infty}^{\infty}R_{m,n,P}f\,(x,y)\ \ \psi_{a,\,b}\,(P)\ dP$$

$$=\frac{1}{8kl}\int_{-\infty}^{\infty}\int_{-l}^{l}\int_{-k}^{k}f\,(x,y)\,\delta\left(\pi\left(P-\frac{m}{k}x-\frac{n}{l}y\right)\right)\psi\left(\frac{t-b}{a}\right)dx\,dy\,dP.$$

$$\left\langle R_{m,n,P}f\,(x,y)\,,\ \psi_{a,\,b}\,(P)\right\rangle=$$

$$\frac{1}{8kl}\int_{-l}^{l}\int_{-k}^{k}f\,(x,y)\left[\int_{-\infty}^{\infty}\delta\left(\pi\left(P-\frac{m}{k}x-\frac{n}{l}y\right)\right)|a|^{-1/2}\ \ \psi\left(\frac{P-b}{a}\right)\ dP\right]dx\,dy \tag{3.2}$$

Assume $\frac{P-b}{a}=c$; (3.2) gives:

$$\left\langle R_{m,n,P}f\,(x,y)\,,\ \psi_{a,\,b}\,(P)\right\rangle$$

$$=\frac{|a|^{-1/2}}{8\pi kl}\int_{-l}^{l}\int_{-k}^{k}f\,(x,y)\left[\int_{-\infty}^{\infty}\delta\left(ac+b-\frac{m}{k}x-\frac{n}{l}y\right)\ \psi\,(c)\ adc\right]dx\,dy. \tag{3.3}$$

From [21, p. 548]

$$\delta\,(ax-y)\ =1/a\delta\,(x-y/a)\,. \tag{3.4}$$

Hence from (3.4), (3.3) gives

$$\left\langle R_{m,n,P}f\,(x,y)\,,\ \psi_{a,\,b}\,(P)\right\rangle$$

$$=\frac{|a|^{-1/2}}{8\pi kl}\int_{-l}^{l}\int_{-k}^{k}f\,(x,y)\left[\int_{-\infty}^{\infty}\delta\left(c-\left(\frac{mx/k\ +ny/l\ -b}{a}\right)\right)\ \psi\,(c)\ dc\right]dx\,dy.$$

Using [19, p. 25] and [20, p. 260], we get

$$\int_{-\infty}^{\infty}f\,(y)\ \delta\,(x-y)\,dy=f\,(x)\,. \tag{3.5}$$

Hence from (3.5), we get

$$\left\langle R_{m,n,P}f\,(x,y)\,,\ \psi_{a,\,b}\,(P)\right\rangle=\frac{|a|^{-1/2}}{8\pi kl}\int_{-l}^{l}\int_{-k}^{k}f\,(x,y)\,\psi\left(\frac{mx/k\ +ny/l\ -b}{a}\right)dx\,dy.$$

Thus follows:

$$\left\langle R_{m,n,P}f\,(x,y)\,,\ \psi_{a,\,b}\,(P)\right\rangle\ =\frac{\pi}{2}\Re_{p/\pi a,q/\pi a,a,b}f\,(x,y)\,. \tag{3.6}$$

□

### 3.2 Representation of finite continuous Radon transform in terms of finite continuous Fourier cosine transform

**Theorem 3.2.** *The finite continuous Radon transform can be represented in terms of finite continuous Fourier cosine transform as:*

$$R_{m,m,m}f(x,y) = \frac{e^{-i\pi m}}{8}\bar{F}_{cc}[f(x,y)] \tag{3.7}$$

*where* $\bar{F}_{cc}[f(x,y)] = \frac{4}{kl}\int_0^l\int_0^k f(x,y)\cos\left(\frac{m\pi}{k}x\right)\cos\left(\frac{n\pi}{l}y\right)dxdy$, *is finite continuous Fourier cosine transform of* $f(x,y)$ *[17].*

*Proof.* Considering (2.3) at $m = n = P$

$$\delta\left(\pi\left(m - \frac{m}{k}x - \frac{n}{l}y\right)\right) = 1 + 2\sum_{m=1}^{\infty}\cos\pi\left(m - \frac{m}{k}x - \frac{m}{l}y\right)$$

further can be written as

$$\begin{aligned}\delta\left(\pi\left(m - \frac{m}{k}x - \frac{m}{l}y\right)\right) &= \sum_{m=-\infty}^{\infty}\cos\pi\left(m - \frac{m}{k}x - \frac{m}{l}y\right)\\ &= e^{\pi\left(m-\frac{m}{k}x-\frac{m}{l}y\right)i}\\ &= e^{\pi mi}\cos\left(\frac{m\pi}{k}x\right)\cos\left(\frac{m\pi}{l}y\right).\end{aligned}$$

Hence

$$\delta\left(\pi\left(m - \frac{m}{k}x - \frac{m}{l}y\right)\right) = e^{\pi mi}\cos\left(\frac{m\pi}{k}x\right)\cos\left(\frac{m\pi}{l}y\right) \tag{3.8}$$

for every $-\infty < m < \infty$ and $-\infty < n < \infty$.
Using (3.8), (2.5) can be written as

$$R_{m,m,m}f(x,y) = \frac{4e^{i\pi m}}{8kl}\int_0^l\int_0^k f(x,y)\cos\left(\frac{m\pi}{k}x\right)\cos\left(\frac{m\pi}{l}y\right)dxdy,$$

$$= \frac{e^{-i\pi m}}{8}\bar{F}_{cc}[f(x,y)]$$

for $m = n$ which proves (3.7). □

### 3.3 Representation of finite continuous Ridgelet transform in terms of finite continuous Fourier cosine transform

**Theorem 3.3.** *The finite continuous Ridgelet transform can be represented in terms of finite continuous Fourier cosine transform as*

$$\Re_{p,q,a,b}f(x,y) = \frac{a^{-1/2}\,e^{b/a}}{4}\bar{F}_{cc}[f(x,y)] \tag{3.9}$$

*where* $\bar{F}_{cc}[f(x,y)] = \frac{4}{\alpha\beta}\int_0^\beta\int_0^\alpha f(x,y)\cos\left(\frac{p'\pi}{\alpha}x\right)\cos\left(\frac{q'\pi}{\beta}y\right)dxdy$, *is finite continuous Fourier cosine transform of* $f(x,y)$ *[17].*

*Proof.* From [18], if $0 < \frac{p}{i} = p' < \infty$, $0 < \frac{q}{i} = q' < \infty$, then (1.4) can be written as

$$\psi\left(\frac{(pa\pi x/\alpha) + (qa\pi y/\beta) - b}{a}\right) = e^{b/a}\,e^{\frac{-ip'\pi}{\alpha}x}e^{\frac{-iq'\pi}{\beta}y}. \tag{3.10}$$

Rewritting (1.2) using (3.10) as

$$\Re_{p,q,a,b} f(x,y) = \frac{a^{-1/2}\, e^{b/a}}{4\alpha\beta} \int_{-\beta}^{\beta}\int_{-\alpha}^{\alpha} f(x,y) \cos\left(\frac{p'\pi}{\alpha}x\right) \cos\left(\frac{q'\pi}{\beta}y\right) dxdy$$

$$= \frac{a^{-1/2}\, e^{b/a}}{4} \bar{F}_{cc}\left[f(x,y)\right].$$

Hence (3.9) proved. □

## 4 Properties of Ridgelet transform

**Lemma 4.1** (Linearity). *The linearity property of Ridgelet transform for $f(x,y)$ and $g(x,y)$ from (1.2) can be stated as:*

$$\Re_{p,q,a,b}\left[cf(x,y) + dg(x,y)\right] = c\Re_{p,q,a,b} f(x,y) + d\Re_{p,q,a,b} g(x,y) \tag{4.1}$$

*where $c$ and $d$ are constants.*

*Proof.* The proof is straight-forward using (1.2). □

**Lemma 4.2** (Shifting). *The shifting property of Ridgelet transform can be stated as:*

$$\Re_{p,q,a,b} f(x-c, y-d) = \Re_{p,q,a,\left(b+\left(\frac{\pi apc}{\alpha}+\frac{\pi aqd}{\beta}\right)\right)} f(x,y) \tag{4.2}$$

$\forall\, x \in (-(\alpha+c),\, (\alpha-d))$ *and* $y \in (-(\beta+c),\, (\beta-d))$.

*Proof.* Using (1.2), and using $x - c = \xi$ and $y - d = \eta$, we get

$$\Re_{p,q,a,b} f(x-c, y-d)$$

$$= \frac{a^{-1/2}}{4\alpha\beta} \int_{-(\beta+d)}^{(\beta+d)}\int_{-(\alpha+c)}^{(\alpha+c)} f(\xi,\eta)\, \psi\left(\frac{\left(\frac{\pi p\xi}{\alpha}+\frac{\pi q\eta}{\beta}\right) - \left(b+\left(\frac{\pi apc}{\alpha}+\frac{\pi aqd}{\beta}\right)\right)}{a}\right) d\xi d\eta.$$

Replacing $\xi$ by $x$ and $\eta$ by $y$, we obtain (4.2). Thus the proof. □

**Lemma 4.3** (Scaling). *The scaling property of Ridgelet transform can be stated as:*

$$\Re_{p,q,a,b} f(cx, dy) = \frac{1}{cd} \Re_{\frac{p}{c},\frac{q}{d},a,b} f(x,y) \tag{4.3}$$

$\forall\, x \in (-c\alpha,\, c\alpha)$ *and* $dy \in (-d\beta,\, d\beta)$.

*Proof.* Let $c > 0$, $d > 0$. For $cx = \xi$, $dy = \eta$, in (1.2) and [18], we get

$$\Re_{p,q,a,b} f(cx, dy) = \frac{a^{-1/2}}{4\alpha\beta} \int_{-\beta}^{\beta}\int_{-\alpha}^{\alpha} f(cx, dy)\, \psi\left(\frac{\left(\frac{\pi px}{\alpha}+\frac{\pi qy}{\beta}\right) - b}{a}\right) dxdy$$

$$= \frac{a^{-1/2}}{4\alpha\beta} \int_{-d\beta}^{d\beta}\int_{-c\alpha}^{c\alpha} f(\xi,\eta)\, \psi\left(\frac{\left(\frac{\pi p\xi}{c\alpha}+\frac{\pi q\eta}{d\beta}\right) - b}{a}\right) \frac{d\xi}{c}\frac{d\eta}{d}.$$

Hence the proof. □

**Lemma 4.4** (Symmetry). *The symmetry property of Ridgelet transform can be stated as:*

*a. First form of symmetric property*

$$\Re_{p,q,ca,db} f(x,y) = c^{-1/2}\, e^{\frac{b}{a}\left(\frac{d}{c}-1\right)} \Re_{p,q,a,b} f(x,y). \tag{4.4}$$

*b. Second form of symmetric property*

$$\Re_{cp,cq,a,b} f(x,y) = \frac{1}{c^2} \Re_{p,q,a,b} f(x,y). \tag{4.5}$$

*Proof.*

a. Using (1.2); we get

$$\Re_{p,q,ca,db} f(x,y) = \frac{ac^{-1/2}}{4\alpha\beta} \int_{-\beta}^{\beta} \int_{-\alpha}^{\alpha} f(x,y)\, \psi\left( \frac{\left(\frac{\pi acpx}{\alpha} + \frac{\pi acqy}{\beta}\right) - bd}{ac} \right) dxdy. \tag{4.6}$$

From [18], we can write

$$\psi\left( \frac{\left(\frac{\pi acpx}{\alpha} + \frac{\pi acqy}{\beta}\right) - bd}{ac} \right) = (ac)^{-1/2}\, e^{\frac{b}{a}\left(\frac{d}{c}-1\right)} \psi\left( \frac{\left(\frac{\pi apx}{\alpha} + \frac{\pi aqy}{\beta}\right) - b}{a} \right). \tag{4.7}$$

Using (4.7) and (4.6) can be written as:

$$\Re_{p,q,ca,db} f(x,y) = \frac{(ac)^{-1/2}\, e^{\frac{b}{a}\left(\frac{d}{c}-1\right)}}{4\alpha\beta} \int_{-\beta}^{\beta} \int_{-\alpha}^{\alpha} f(x,y)\, \psi\left( \frac{\left(\frac{\pi apx}{\alpha} + \frac{\pi aqy}{\beta}\right) - b}{a} \right) dxdy$$

$$= c^{-1/2}\, e^{\frac{b}{a}\left(\frac{d}{c}-1\right)} \Re_{p,q,a,b} f(x,y)$$

which is the required proof.

b. Representing (1.2) as:

$$\Re_{cp,cq,a,b} f(x,y) = \frac{a^{-1/2}}{4\alpha\beta} \int_{-\beta}^{\beta} \int_{-\alpha}^{\alpha} f(x,y)\, \psi\left( \frac{\left(\frac{\pi acpx}{\alpha} + \frac{\pi acqy}{\beta}\right) - b}{a} \right) dxdy.$$

Let $cx = \xi$, $cy = \eta$, we get

$$\Re_{cp,cq,a,b} f(x,y) = \frac{a^{-1/2}}{4\alpha\beta} \int_{-c\beta}^{c\beta} \int_{-c\alpha}^{c\alpha} f(\xi,\eta)\, \psi\left( \frac{\left(\frac{\pi p\xi}{\alpha} + \frac{\pi q\eta}{\beta}\right) - b}{a} \right) \frac{d\xi d\eta}{c^2}.$$

Replacing $\xi$ by $x$ and $\eta$ by $y$, we obtain (4.5).
Hence the proof.

□

## 5 Properties of Radon transform

**Lemma 5.1** (Linearity). *If $R_{m,n,P} f(x,y)$ and $R_{m,n,P} g(x,y)$ are finite continuous Radon transform for $f(x,y)$ and $g(x,y)$, then linearity property of can be stated as:*

$$R_{m,n,P}\left[a f(x,y) + b g(x,y)\right] = a R_{m,n,P} f(x,y) + b R_{m,n,P} g(x,y) \tag{5.1}$$

*where $a$ and $b$ are constants.*

*Proof.* The proof is straight-forward using (2.5). □

**Lemma 5.2** (Shifting). *The shifting property of finite continuous Radon transform can be stated as:*

$$R_{m,n,P} f(x-a,\, y-b) = R_{m,n,\left(P - \frac{m}{k}a - \frac{n}{l}b\right)} f(x,\, y). \tag{5.2}$$

$\forall\, x \in (-(k+a),\, (k-a))$ *and* $y \in (-(l+b),\, (l-b))$.

*Proof.* From (2.5) and using $x-a=\xi$ and $y-b=\eta$, we get

$$R_{m,n,P}f\,(x-a,\,y-b)$$
$$=\frac{1}{8kl}\int_{-(l+b)}^{(l-b)}\int_{-(k+a)}^{(k-a)} f\,(\xi,\,\eta)\,\delta\left(\pi\left(P-\frac{m}{k}\,(\xi+a)-\frac{n}{l}\,(\eta+b)\right)\right)d\xi d\eta$$
$$=\frac{1}{8kl}\int_{-(l+b)}^{(l-b)}\int_{-(k+a)}^{(k-a)} f\,(\xi,\,\eta)\,\delta\left(\pi\left(\left(P-\frac{m}{k}a-\frac{n}{l}b\right)-\frac{m}{k}\xi-\frac{n}{l}\eta\right)\right)d\xi d\eta.$$

Replacing $\xi$ by $x$ and $\eta$ by $y$, we obtain

$$R_{m,n,P}f\,(x-a,\,y-b)=R_{m,n,\left(P-\frac{m}{k}a-\frac{n}{l}b\right)}f\,(x,\,y)\,.$$

□

**Lemma 5.3** (Scaling). *The scaling property of finite continuous Radon transform can be stated as:*

$$R_{m,n,P}f\,(ax,by)=\frac{1}{ab}R_{\frac{m}{a},\frac{n}{b},P}f\,(x,y) \tag{5.3}$$

$\forall\, x\in(-ak,\,ak)$ *and* $y\in(-bl,\,bl)$.

*Proof.* Let $a>0$, $b>0$. For $ax=\xi$, $by=\eta$, and (2.5), we have

$$R_{m,n,P}f\,(ax,by)=\frac{1}{8kl}\int_{-l}^{l}\int_{-k}^{k} f\,(ax,by)\,\delta\left(\pi\left(P-\frac{m}{k}x-\frac{n}{l}y\right)\right)dxdy$$
$$=\frac{1}{8kl}\int_{-bl}^{bl}\int_{-ak}^{ak} f\,(\xi,\eta)\,\delta\left(\pi\left(P-\frac{m}{ak}\xi-\frac{n}{bl}\eta\right)\right)\frac{d\xi}{a}\frac{d\eta}{b}$$

and hence the scaling lemmaperty holds true. □

**Lemma 5.4** (Symmetric). *The symmetric property of finite continuous Radon transform can be stated as:*

*a. First form of symmertic property*

$$R_{am,an,aP}f\,(x,\,y)=\frac{1}{|a|}R_{m,n,P}f\,(x,\,y)\,. \tag{5.4}$$

*b. Second form of symmertic property*

$$R_{am,an,P}f\,(x,\,y)=\frac{1}{|a|}R_{m,n,\frac{P}{a}}f\,(x,\,y)\,. \tag{5.5}$$

*Proof.*

a. Using (2.5) and (3.4), first form of symmetric property is given by:

$$R_{am,an,aP}f\,(x,\,y)=\frac{1}{8\,|a|\,kl}\int_{-l}^{l}\int_{-k}^{k} f\,(x,y)\,\delta\left(\pi\left(P-\frac{m}{k}x-\frac{n}{l}y\right)\right)dxdy$$
$$=\frac{1}{|a|}R_{m,n,P}f\,(x,\,y)$$

which is the required proof.

b. Second form of symmetric property, using (2.5) and (3.4) is

$$R_{am,an,P}f\left(x,\,y\right)=\frac{1}{8kl}\int_{-l}^{l}\int_{-k}^{k}f\left(x,y\right)\delta\left(\pi\left(P-\frac{am}{k}x-\frac{an}{l}y\right)\right)dxdy$$

$$=\frac{1}{8\left|a\right|kl}\int_{-l}^{l}\int_{-k}^{k}f\left(x,y\right)\delta\left(\pi\left(\frac{P}{a}-\frac{m}{k}x-\frac{n}{l}y\right)\right)dxdy$$

$$=\frac{1}{|a|}R_{m,n,\frac{P}{a}}f\left(x,\,y\right).$$

Thus the symmetric property holds true. □

## 6 Application

**Example 6.1.** The network trained to map the $f\left(x,y\right)=e^{\left(-(x-2)^2-(y-1.5)^2\right)}-e^{\left(-(x-4)^2-(y-4)^2\right)}$ occur in neural network during data stream processing as in [14], find the Ridgelet transform of such a function.
The Ridgelet transform of this function
$f\left(x,y\right)=e^{\left(-(x-2)^2-(y-1.5)^2\right)}-e^{\left(-(x-4)^2-(y-4)^2\right)}$, using (3.6) is given by:

$$\Re_{p,q,a,b}f\left(x,y\right)=\frac{2}{\pi}\int_{-\infty}^{\infty}R_{m,n,P}\left[e^{\left(-(x-2)^2-(y-1.5)^2\right)}-e^{\left(-(x-4)^2-(y-4)^2\right)}\right]\psi_{a,\,b}\left(t\right)\,dt\,. \quad (6.1)$$

From (2.5)

$$R_{m,n,P}\left[e^{\left(-(x-2)^2-(y-1.5)^2\right)}-e^{\left(-(x-4)^2-(y-4)^2\right)}\right]$$

$$=\frac{1}{8kl}\int_{-l}^{l}\int_{-k}^{k}\left[e^{\left(-(x-2)^2-(y-1.5)^2\right)}-e^{\left(-(x-4)^2-(y-4)^2\right)}\right]\delta\left(\pi\left(P-\frac{m}{k}x-\frac{n}{l}y\right)\right)dxdy. \quad (6.2)$$

From (3.5), we get

$$R_{m,n,P}f\left(x,y\right)=\frac{p}{8\pi lmn}\left[e^{\left(-(kp/m\,-2)^2-3\right)}-e^{\left(-(kp/m\,-4)^2-16\right)}\right]. \quad (6.3)$$

Using (6.3), (6.1) can be represented as:

$$\Re_{p,q,a,b}f\left(x,y\right)\;=\;\frac{p}{4\pi^2lmn}\int_{-\infty}^{\infty}\left[e^{\left(-(kp/m\,-2)^2-3\right)}-e^{\left(-(kp/m\,-4)^2-16\right)}\right]\psi_{a,\,b}\left(t\right)\,dt\,. \quad (6.4)$$

Consider $\psi_{a,\,b}\left(t\right)=\left(1-t^2\right)\,e^{-at^2/2}$ which is a Mexican Hat wavelet [21] for $a=1$, (6.4) is obtained as:

$$\Re_{p,q,a,b}f\left(x,y\right)\;=\;\frac{p}{4\pi^2lmn}\int_{-\infty}^{\infty}\left[e^{\left(-(kt/m\,-2)^2-3\right)}-e^{\left(-(kt/m\,-4)^2-16\right)}\right]\left(1-t^2\right)\,e^{-t^2/2}\,dt. \quad (6.5)$$

$$\Re_{p,q,a,b}f\left(x,y\right)\;=\;\frac{p}{8e^{16}\pi^{3/4}\,lkn}\left\{\begin{array}{l}erf\left(4-kl/m\,\right)-erf\left(kl/m\,+4\right)\\+e^{13}\left(erf\left(kl/m\,+2\right)+erf\left(kl/m\,-2\right)\right)\end{array}\right\}. \quad (6.6)$$

The example 6.1 concludes that using relation between finite continuous Radon and Ridgelet transform, the neural network function $f(x,y) = e^{\left(-(x-2)^2-(y-1.5)^2\right)} - e^{\left(-(x-4)^2-(y-4)^2\right)}$ can be converted to finite continuous Ridgelet transform which gives a clear 3D view of this network. The FIGURES 1 and 2, shows the plot of $e^{\left(-(x-2)^2-(y-1.5)^2\right)} - e^{\left(-(x-4)^2-(y-4)^2\right)}$, whereas imposing finite continuous Ridgelet transform on the network which is given by (6.6), the FIGURES are represented as 3 and 4.

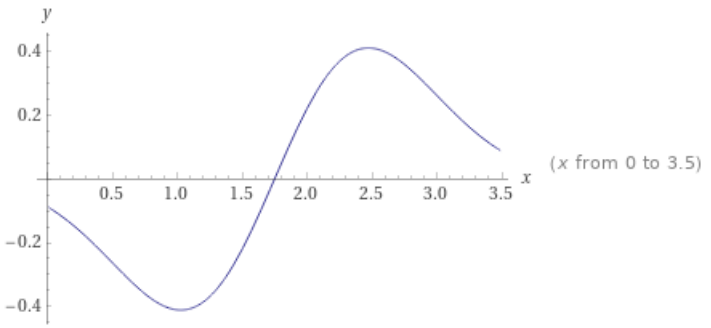



**Figure 1.** Plot of the networks $f(x,y) = e^{\left(-(x-2)^2-(y-1.5)^2\right)} - e^{\left(-(x-4)^2-(y-4)^2\right)}$ without finite continuous Ridgelet transform

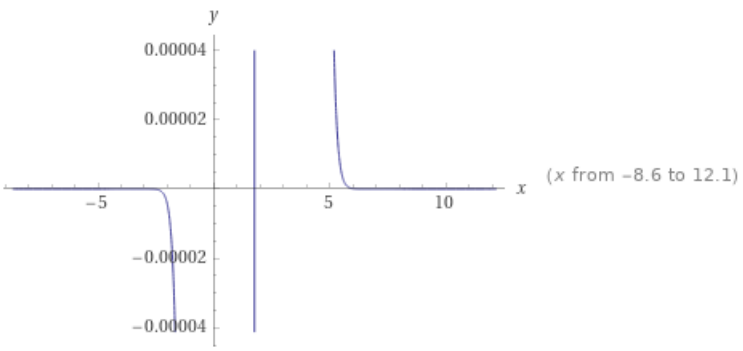



**Figure 2.** Plot of the networks $f(x,y) = e^{\left(-(x-2)^2-(y-1.5)^2\right)} - e^{\left(-(x-4)^2-(y-4)^2\right)}$ without finite continuous Ridgelet transform

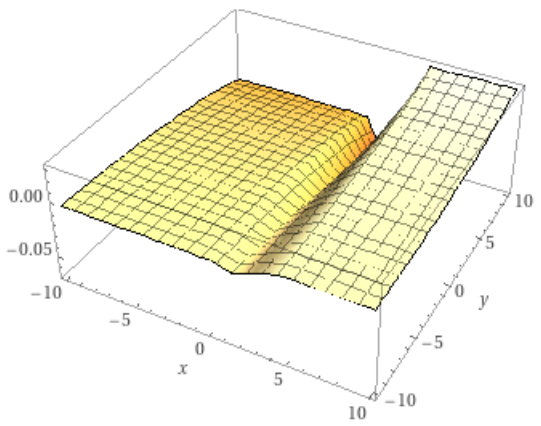



**Figure 3.** 3D plot: Finite continuous Ridgelet transform on the networks trained to map

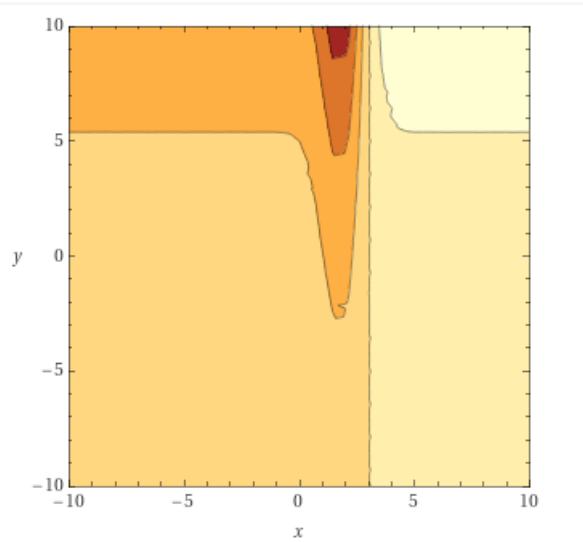



**Figure 4.** Contour plot: Finite continuous Ridgelet transform on the networks trained to map

**Example 6.2.** Application of finite continuous Radon transform and finite continuous Ridgelet transform to Klein-Gordon equation of linear non-homogeneous form:
Considering the linear non-homogeneous Klein-Gordon equation for any scalar field $u$, with initial conditions [16]

$$u_{tt} - u_{xx} + u = -x\cos t + x^2\cos^2 t; \tag{6.7}$$

$$u_0(x,0) = x, u_t(x,0) = 0. \tag{6.8}$$

i. To solve the initial value problem, applying finite continuous Radon transform (2.5) on both the sides of (6.7), we get

$$R_{m,n,P}\left[\frac{\partial^2 u}{\partial t^2}\right] - R_{m,n,P}\left[\frac{\partial^2 u}{\partial x^2}\right] + R_{m,n,P}u = -\cos t R_{m,n,P}[x] + \cos^2 t R_{m,n,P}\left[x^2\right]. \tag{6.9}$$

Using (2.7) and (2.8)

$$\frac{\partial^2 \bar{U}}{\partial t^2} - \left[\left(\frac{m\pi}{k}\right)^2 - 1\right]\bar{U} = -\cos t\, C + \cos^2 t\, D; \tag{6.10}$$

where $\bar{U} = R_{m,n,P}u(x,y) = \frac{1}{8kl}\int_{-l}^{l}\int_{-k}^{k} u(x,y)\,\delta\left(\pi\left(P - \frac{m}{k}x - \frac{n}{l}y\right)\right)dxdy$ and $C = R_{m,n,P}[x] =$ constant and $D = R_{m,n,P}\left[x^2\right] =$ constant.
Similarly applying finite continuous Radon transform on both sides of (6.8), we get

$$\bar{U}(x,0) = C, \bar{U}_t(x,0) = 0. \tag{6.11}$$

Solving (6.10), using (6.11), we get

$$\bar{U} = A\left(e^{-\left(\sqrt{\left(\frac{m\pi}{k}\right)^2 - 1}\right)t} + e^{\left(\sqrt{\left(\frac{m\pi}{k}\right)^2 - 1}\right)t}\right) - \frac{\cos t}{\left(\frac{m\pi}{k}\right)^2} + \frac{1}{2}\left(\frac{\cos 2t}{\left(\left(\frac{m\pi}{k}\right)^2 + 3\right)} - \frac{1}{\left(\left(\frac{m\pi}{k}\right)^2 - 1\right)}\right) \tag{6.12}$$

where $A = \frac{1}{2}\left[C + \frac{1}{\left(\frac{m\pi}{k}\right)^2} - \left(\frac{1}{\left(\left(\frac{m\pi}{k}\right)^2 + 3\right)} + \frac{1}{\left(\left(\frac{m\pi}{k}\right)^2 - 1\right)}\right)\right]$.
We may now invoke the inversion formula (2.6) to provide the required result

$$u(x,t) = \sum_{m=1,n=1}^{\infty} \left[ A\left( e^{-\left(\sqrt{\left(\frac{m\pi}{k}\right)^2-1}\right)t} + e^{\left(\sqrt{\left(\frac{m\pi}{k}\right)^2-1}\right)t} \right) - \frac{\cos t}{\left(\frac{m\pi}{k}\right)^2} + \frac{1}{2}\left( \frac{\cos 2t}{\left(\left(\frac{m\pi}{k}\right)^2+3\right)} - \frac{1}{\left(\left(\frac{m\pi}{k}\right)^2-1\right)} \right) \right] \delta\left(\pi\left(P - \frac{m}{k}x - \frac{n}{l}y\right)\right). \tag{6.13}$$

ii. Similarly (6.7)-(6.7) can be solved using finite continuous Ridgelet transform (1.2), using $\Re_{p,q,a,b}\left\{\frac{\partial^2 f}{\partial x^2}\right\} = \left(\frac{p\pi}{\alpha}\right)^2 \Re_{p,q,a,b} f(x,y)$ from [18] and (1.3), we obtain the result

$$u(x,t) = a^{1/2} \sum_{p,q=1}^{\infty} \left[ E\left( e^{-\left(\sqrt{\left(\frac{p\pi}{\alpha}\right)^2-1}\right)t} + e^{\left(\sqrt{\left(\frac{p\pi}{\alpha}\right)^2-1}\right)t} \right) - \frac{\cos t}{\left(\frac{p\pi}{\alpha}\right)^2} + \frac{1}{2}\left( \frac{\cos 2t}{\left(\left(\frac{p\pi}{\alpha}\right)^2+3\right)} - \frac{1}{\left(\left(\frac{p\pi}{\alpha}\right)^2-1\right)} \right) \right] \psi\left( \frac{\left(\frac{\pi apx}{\alpha} + \frac{\pi aqy}{\beta}\right) - b}{a} \right) \tag{6.14}$$

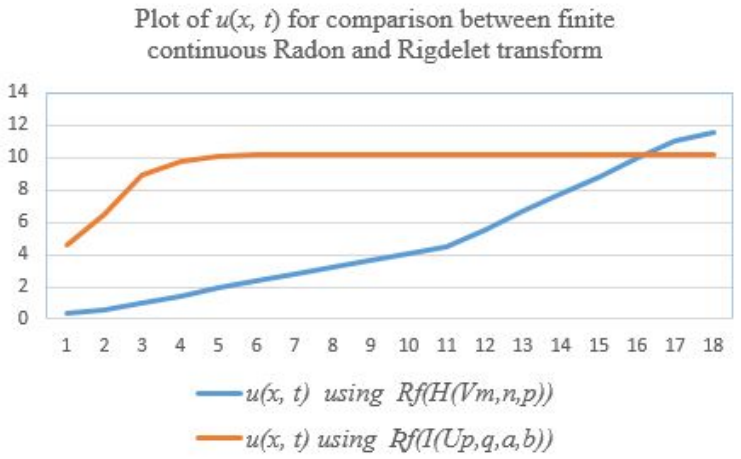
where $E = A = \frac{1}{2}\left[F + \frac{1}{\left(\frac{p\pi}{\alpha}\right)^2} - \left(\frac{1}{\left(\left(\frac{p\pi}{\alpha}\right)^2+3\right)} + \frac{1}{\left(\left(\frac{p\pi}{\alpha}\right)^2-1\right)}\right)\right]$ and $F = \Re_{p,q,a,b}[x] =$ constant.

In TABLE 1, numerical value of $u(x,t)$ at different order of $m \times n$ or $p \times q$ using finite continuous Radon and Ridgelet transform is studied. The comparison graph shown in FIGURE 5 indicates that the value of $u(x,t)$, when computed using the finite continuous Radon transform, continues to increase. In contrast, the value obtained using the finite continuous Ridgelet transform tends to saturate, particularly at $40 \times 40$.

**Table 1.** Numerical value of $u(x,t)$, using finite continuous Radon and Ridgelet transform at $k = l = \alpha = \beta = 10$

| $m \times n / p \times q$ | $u(x,t)$ fron (6.13) at $p = 500$ | $u(x,t)$ from (6.14) at $a = b = 4000$ |
|---|---|---|
| $2 \times 2$ | 0.48 | 4.5578 |
| $4 \times 4$ | 0.6118 | 6.5066 |
| $8 \times 8$ | 1.0415 | 8.8906 |
| $12 \times 12$ | 1.474 | 9.7899 |
| $16 \times 16$ | 1.9083 | 10.0715 |
| $20 \times 20$ | 2.3424 | 10.1540 |
| $24 \times 24$ | 2.7754 | 10.1540 |
| $28 \times 28$ | 3.2080 | 10.1778 |
| $32 \times 32$ | 3.6415 | 10.1846 |
| $36 \times 36$ | 4.076 | 10.187 |
| $40 \times 40$ | 4.5107 | 10.1872 |
| $50 \times 50$ | 5.593 | 10.1873 |
| $60 \times 60$ | 6.6795 | 10.1873 |
| $70 \times 70$ | 7.7622 | 10.1873 |
| $80 \times 80$ | 8.8485 | 10.1873 |
| $90 \times 90$ | 9.9311 | 10.1873 |
| $100 \times 100$ | 11.0174 | 10.1873 |
| $110 \times 110$ | 12.1001 | 10.1873 |

**Figure 5.** $u(x,t)$: comparison between finite continuous Radon and Rigdelet transform using (6.13) and (6.14)




**Example 6.3.** Application of finite continuous Ridgelet transform finite continuous Radon transform to Klein-Gordon equation of linear non-homogeneous form:
Considering the linear non-homogeneous Klein-Gordon equation for any scalar field $v$, with initial conditions [16]

$$v_{tt} - v_{xx} - 2v = -2\cos x \cos t; \tag{6.15}$$

$$v(x,0) = 0, v_t(x,0) = \cos x. \tag{6.16}$$

i. To solve the initial value problem (6.15), applying finite continuous Ridgelet transform (1.2) on both sides, we get

$$\Re_{p,q,a,b}\left[\frac{\partial^2 v}{\partial t^2}\right] - \Re_{p,q,a,b}\left[\frac{\partial^2 v}{\partial x^2}\right] - 2\Re_{p,q,a,b} v(x,y) = -2\cos t\, \Re_{p,q,a,b} \cos x. \tag{6.17}$$

The linear non-homogeneous Klein-Gordon equation can be further solved by using $\Re_{p,q,a,b}\left\{\frac{\partial^2 f}{\partial x^2}\right\} = \left(\frac{p\pi}{\alpha}\right)^2 \Re_{p,q,a,b} f(x,y)$ from [18] as:

$$\frac{\partial^2 \bar{V}}{\partial t^2} - \left(\left(\frac{p\pi}{\alpha}\right)^2 + 2\right)\bar{V} = -2C_1 \cos t, \tag{6.18}$$

where $\bar{V} = \Re_{p,q,a,b} u(x,y) = \frac{a^{-1/2}}{4\alpha\beta} \int_{-\beta}^{\beta}\int_{-\alpha}^{\alpha} v(x,y)\, \psi\left(\frac{\left(\frac{\pi a p x}{\alpha} + \frac{\pi a q y}{\beta}\right) - b}{a}\right) dxdy$
and $C_1 = \Re_{p,q,a,b} \cos x = \text{constant}$.
Also finite continuous Ridgelet transform on both the sides of(6.16), we obtain:

$$\bar{V}(x,0) = 0, \bar{V}_t(x,0) = C_1. \tag{6.19}$$

Equation (6.18) is second order differential equation, whose solution is given by

$$\bar{V} = A_1 e^{-\left(\sqrt{\left(\frac{p\pi}{\alpha}\right)^2 + 2}\right)t} + B_1 e^{\left(\sqrt{\left(\frac{p\pi}{\alpha}\right)^2 + 2}\right)t} + \frac{2C_1 \cos t}{\left(\frac{p\pi}{\alpha}\right)^2 + 3}. \tag{6.20}$$

To find constants $A_1$ and $B_1$, applying the conditions (6.19), we obtain

$$\bar{V} = \frac{C_1}{2\sqrt{\left(\frac{p\pi}{\alpha}\right)^2 + 3}}\left[-e^{-\left(\sqrt{\left(\frac{p\pi}{\alpha}\right)^2 + 2}\right)t} + e^{\left(\sqrt{\left(\frac{p\pi}{\alpha}\right)^2 + 2}\right)t} + \frac{4C_1 \cos t}{\sqrt{\left(\frac{p\pi}{\alpha}\right)^2 + 3}}\right]. \tag{6.21}$$

We may now invoke the inversion formula (1.3) to provide the required result as:

$$v(x,t) = a^{1/2} \sum_{p=1,q=1}^{\infty} \frac{C_1}{2\sqrt{\left(\frac{p\pi}{\alpha}\right)^2+3}} \left[ -e^{-\left(\sqrt{\left(\frac{p\pi}{\alpha}\right)^2+2}\right)t} + e^{\left(\sqrt{\left(\frac{p\pi}{\alpha}\right)^2+2}\right)t} + \frac{4C_1 \sin t}{\sqrt{\left(\frac{p\pi}{\alpha}\right)^2+3}} \right] \times \psi\left( \frac{\left(\frac{\pi apx}{\alpha} + \frac{\pi aqy}{\beta}\right) - b}{a} \right). \tag{6.22}$$

ii. Similarly applying finite continuous Radon transform from (2.5) to (6.13) and (6.14), using the operator from (2.7) and (2.8) then applying the inversion formula (2.6), we obtain

$$v(x,t) = \sum_{m=1,n=1}^{\infty} \frac{G}{2\sqrt{\left(\frac{m\pi}{k}\right)^2+3}} \left[ -e^{-\left(\sqrt{\left(\frac{m\pi}{k}\right)^2+2}\right)t} + e^{\left(\sqrt{\left(\frac{m\pi}{k}\right)^2+2}\right)t} + \frac{4G \sin t}{\sqrt{\left(\frac{m\pi}{k}\right)^2+3}} \right] \times \delta\left(\pi\left(P - \frac{m}{k}x - \frac{n}{l}y\right)\right) \tag{6.23}$$

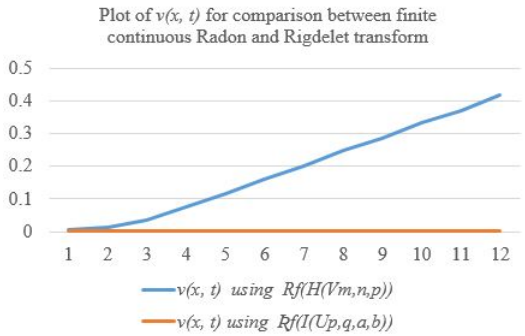
where $G = R_{m,n,P}[\cos x] =$ constant.

The numerical value of $v(x,t)$ at different order of $m \times n$ or $p \times q$ using finite continuous Radon and Ridgelet transform is studied in TABLE 2. The comparison graph given in FIGURE 6 concludes that the value of $v(x,t)$ using finite continuous Radon transform increases, while the value of $v(x,t)$ using finite continuous Ridgelet transform value reaches saturation level after $p \times q$ at $20 \times 20$.

**Table 2.** Numerical value of $v(x,t)$, using finite continuous Radon and Ridgelet transform at $k = l = \alpha = \beta = 10$

| $m \times n$ /$p \times q$ | $v(x,t)$ using (6.22) at $p = 1$ | $v(x,t)$ using (6.23) at $a = b = 400$ |
|---|---|---|
| $2 \times 2$ | 0.00613 | 0.00075 |
| $4 \times 4$ | 0.01435 | 0.0011 |
| $10 \times 10$ | 0.03376 | 0.001166 |
| $20 \times 20$ | 0.0773 | 0.001167 |
| $30 \times 30$ | 0.1175 | 0.001167 |
| $40 \times 40$ | 0.16217 | 0.001167 |
| $50 \times 50$ | 0.2022 | 0.001167 |
| $60 \times 60$ | 0.2470 | 0.001167 |
| $70 \times 70$ | 0.2870 | 0.001167 |
| $80 \times 80$ | 0.3319 | 0.001167 |
| $90 \times 90$ | 0.3718 | 0.001167 |
| $100 \times 100$ | 0.4167 | 0.001167 |

**Figure 6.** $v(x,t)$: comparison between finite continuous Radon and Rigdelet transform




## 7 Conclusion remarks

The study presents the relationship between the finite continuous Radon and Ridgelet transforms. Both transforms are represented in terms of the finite continuous Fourier transform. The concluding section includes applications and graphical representations involving a neural network that uses the Mexican Hat wavelet. Additionally, the study demonstrates an application to a neural network based on the solutions of two different forms of the linear non-homogeneous Klein-Gordon equation with their respective initial conditions. This study also checks the validity of the newly developed finite continuous Radon and Ridgelet transforms, which are better suited for certain types of data and problems, especially those involving geometric features like lines, edges, or ridges in multi-dimensional data.

## References

[1] J. Radon, *On the determination of functions from their integrals along certain manifolds*, IEEE Transactions on Medical Imaging, **5**, 262-277, (1986).

[2] E.J. Candés, *Harmonic analysis of neural networks*, Technical report, Department of Statistics. University of Stanford, **6**(2), 197-218, (1996).

[3] O. Tretiak and C. Metz, *The exponential Radon transform*, SIAM Journal on Applied Mathematics, **39**, 341-354, (1980).

[4] T.S. Durrani, and D. Bisset, *The Radon transform and its properties*. Geophysics, **49**, 1180-1187, (1984).

[5] J. He and H. Liu, *Inversion of the Radon transform associated with the classical domain of type one*, Int. J. Math, **16**, 875–887, (2005).

[6] A. Seeger, *Radon transforms and finite type conditions*, Journal of the American Mathematical Society, **11**, 869-897, (1998).

[7] M. Revers,*Numerical integration of the radon transform on classes $E_s^\alpha$ in multiple (finite) dimensions*, Computing, **54**, 147-165, (1995).

[8] H. Choi, V. Ginting, F. Jafari and R. Mnatsakanov, *Modified Radon transform inversion using moments*, Journal of Inverse and Ill-posed Problems, **28**, 1-15, (2019).

[9] N. Murata, An Integral Representation of Functions Using Three-layered Networks and Their Approximation Bounds, Neural Networks, **9**, 947-956, (1996).

[10] D. Donoho, Orthonormal ridgelets and linear singularities SIAM Journal on Mathematical Analysis, **31**, 1062-1099, (2000).

[11] E.J. Candés and D.L. Donoho, *Ridgelets: A key to higher-dimensional intermittency?"*, Philosophical Transactions of the Royal Society of London, Series A: Mathematical, Physical and Engineering Sciences, **1760**, 2495-2509, (1999).

[12] L. Akila and R. Roopkumar, *Ridgelet transform for quarternion-valued functions. International Journal of Wavelets*, Multiresolution and Information Processing, **14**, 1650006, (2016).

[13] M.N. Do and M. Vetterli, *The finite ridgelet transform for image representation* IEEE Transactions on image Processing, **12**, 16-28 (2003).

[14] S. Sonoda, I. Ishikawa, M. Ikeda, K. Hagihara, Y. Sawano, T. Matsubara and N. Murata, *The global optimum of shallow neural network is attained by ridgelet transform*, arXiv preprint arXiv. **1805.07517**, (2018).

[15] M. A. AL-Gwaiz, *Stum-Liouville Theory and its Applications*, London: Springer, (2008).

[16] M.S.H Chowdhury and I. Hashim, *Application of homotopy-perturbation method to Klein–Gordon and sine-Gordon equations*. Chaos, Solitons & Fractals. **39**, 1928-1935, (2009).

[17] I.N. Sneddon, *The use of integral transforms*' McGraw-Hill, Inc., (1972).

[18] N. Gupta and V.R.L. Gorty, *Finite Continuous Ridgelet Transforms with Applications to Telegraph and Heat Conduction*, Advances in Dynamical Systems and Applications. **15**, 83-100, (2020).

[19] R.P. Kanwal, *Generalized functions theory and technique: Theory and technique*, Springer Science & Business Media, (2012).

[20] A.G. Ramm, and A.I. Katsevich, *The Radon transform and local tomography*, Boca Raton: CRC press,( 1996).

[21] L. Debnath and D. Bhatta, *Integral transforms and their applications*, Chapman and Hall/CRC press, Taylor & Francis Group's journal, (2006).

[22] H.G. Lee and V. Kim, *Regularized Dirac delta functions for phase-field models*, International Journal for Numerical Methods in Engineering, **91**, 269-288, (2012).

[23] N. Cangiotti, M. Caponi, A. Maione and E. Vitillaro, Klein-Gordon-Maxwell equations driven by mixed local-nonlocal operators. Milan J. Math. (2023).

[24] N. Gupta and V.R.L. Gorty, *Finite continuous Radon transforms with applications*, Advances in Dynamical Systems and Applications. **62**, 69-81, (2024).

[25] A. B. Deshi and G. A. Gudodagi, *The numerical solution of hyperbolic differential equations using Wavelet lifting scheme*, Palestine Journal of Mathematics. **12**, 26-33, (2023).

[26] S. Q. Hasan, U. M. Abubakar and M. L. Kaurangini, *The New Integral Transform "SUM Transform" and Its Properties*, Palestine Journal of Mathematics. **12(Special Issue I)**, 30-45, (2023).

[27] J. E. Nápoles Valdes, *On an integral transformation for Generalized Differential Equations*, Palestine Journal of Mathematics. **13**, 150-163, (2024).

## Author information

N. Gupta, Mukesh Patel School of Technology Management & Engineering, SVKM's NMIMS, Mumbai, India.
E-mail: nitu.gupta@nmims.edu

V. R. Lakshmi Gorty, Mukesh Patel School of Technology Management & Engineering, SVKM's NMIMS, Mumbai, India.
E-mail: vr.lakshmigorty@nmims.edu

Received: 2024-05-01.
Accepted: 2026-04-29.